

High-resolution angle-resolved photoemission study of the Fermi surface and the normal-state electronic structure of $\text{Bi}_2\text{Sr}_2\text{CaCu}_2\text{O}_8$

C. G. Olson, R. Liu, and D. W. Lynch

Ames Laboratory and Physics Department, Iowa State University, Ames, Iowa 50011

R. S. List and A. J. Arko

Los Alamos National Laboratory, Los Alamos, New Mexico 87545

B. W. Veal, Y. C. Chang, P. Z. Jiang, and A. P. Paulikas

Argonne National Laboratory, Argonne, Illinois 60439

(Received 21 December 1989)

High-resolution angle-resolved photoelectron spectroscopic measurements were made of the Fermi edge of a single crystal of $\text{Bi}_2\text{Sr}_2\text{CaCu}_2\text{O}_8$ at 90 K along several directions in the Brillouin zone. The resultant Fermi-level crossings are consistent with local-density band calculations, including a point calculated to be of Bi-O character. Additional measurements were made where bands crossed the Fermi level between 100 and 250 K, along with measurements on an adjacent Pt foil. The Fermi edges of both materials agree to within the noise. Below the Fermi level the spectra show correlation effects in the form of an increased effective mass, but the essence of the single-particle band structure is retained. The shape of the spectra can be explained by a lifetime-broadened photohole and secondary electrons. The effective inverse photohole lifetime is linear in energy.

I. INTRODUCTION

Since the discovery of high- T_c superconductors, their electronic structure has been of great interest. Whether or not the normal states of these materials are Fermi liquids has been a key question. Is one-electron band theory adequate as a starting point for describing the normal-state electronic structure (with added modifications from correlation effects) or must an alternative description be devised?^{1,2} Answers to these questions are important for the ultimate understanding of the mechanism of superconductivity in these materials.

In an attempt to address some of these questions, we carried out a detailed angle-resolved photoemission study on normal-state $\text{Bi}_2\text{Sr}_2\text{CaCu}_2\text{O}_8$. The experiment was performed with high energy and angular resolution, a prerequisite for studying the details of the states near the Fermi level. To minimize thermal broadening, measurements were made at temperatures just above T_c .

An angle-resolved photoemission study on high- T_c superconductors is simplified by the fact that most of the structures are highly two dimensional. In the photoemission process momentum parallel to the surface is conserved. Momentum perpendicular to the surface is not conserved since the photoelectron transfers a certain perpendicular momentum to the crystal when escaping through the surface barrier. For a two-dimensional system, however, the momentum parallel to the surface is sufficient to determine the initial state.

Previous measurements on $\text{Bi}_2\text{Sr}_2\text{CaCu}_2\text{O}_8$ (Ref. 3) showed that bands are negligibly dispersive in the direction normal to the a - b plane, consistent with the two-dimensionality. By measuring photoelectron energy dis-

tribution curves (EDC's) at 90 K (above T_c) as a function of angle, we were able to isolate a single band dispersing through the Fermi level, and determine the point in the Brillouin zone where the band crosses the Fermi level. The measurement is accurate to 2° . (For 22 eV photon energy, this corresponds to $\Delta k_{\parallel} = 0.075 \text{ \AA}^{-1}$.) Such measurements were made along major symmetry lines. The basic features of the Fermi surface were obtained. The results will be presented and discussed in three sections: band dispersion and the Fermi surface, a more detailed analysis of the spectral line shapes, and a comparison of the filled states at the Fermi level to a conventional Fermi liquid.

II. EXPERIMENTAL

A single crystal of $\text{Bi}_2\text{Sr}_2\text{CaCu}_2\text{O}_8$ was cleaved at 20 K in a vacuum better than 5×10^{-11} Torr. The surface was a (001) plane.⁴ Previous work with the 1:2:3 compounds^{5,6} showed that the surface layers sampled by photoelectron spectroscopy degraded rapidly at 50 K, but the Bi compounds proved to be much more stable. Samples cleaved in ultrahigh vacuum at 20 K could be cycled to 90 K and back without detectable changes in the photoelectron spectrum. The samples were stable unless held at room temperature for many hours. The sample used had a value of T_c of 82 K determined from dc SQUID magnetization measurements. Photons were provided by the Ames/Montana ERG/Seya beam line on Aladdin,⁷ using the Seya in the 15–25 eV region. The instrument function of the monochromator was measured. The FWHM is 24 meV for 22 eV photons. The photoelectrons were energy analyzed by a 50 mm radius hemi-

spherical analyzer. The analyzer has a Gaussian instrument function with a FWHM of 20 meV at the pass energy of 2 eV, and 50 meV at a pass energy of 5 eV. The combined instrument function (FWHM 32 meV and 55 meV, respectively) was verified by measurement of a metallic Fermi level at 20 K. Note that this resolution is equal to, or better than, the width of the Fermi-Dirac function (4.4 kT) over the temperatures of the scans we report here. The analyzer input lens had an angular acceptance of about 2°. In the spectra to be reported the energy scale is that of the initial state (“binding energy”).

III. RESULTS AND DISCUSSION

A. Band dispersion and Fermi surface

The spectra shown in Fig. 1 are taken at 90 K along a line parallel to Γ -Y (their positions in the Brillouin zone are shown as solid dots in Fig. 2), with 22 eV photon energy. It can be seen that a band disperses toward the Fermi level from at least 350 meV below E_F . At 12°, the Lorentzian peak is cut off by the Fermi-Dirac function, and the leading edge coincides with the Pt edge. This is a clear indication that the band has just crossed the Fermi level at this point. As indicated in Fig. 2, the 12° point almost falls on the Fermi surface predicted by band calculations.^{8,9} At 14°, the band has completely passed the Fermi level. The details of the spectral shapes will be discussed in the next section.

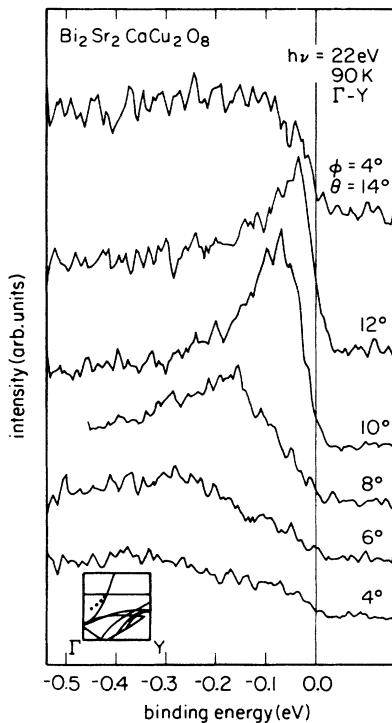


FIG. 1. Angle-resolved energy distribution curves for several angles along the Γ -Y direction in the Brillouin zone using photons of energy 22 eV. The inset shows the measured band dispersion (dots) and the calculated bands from Ref. 8.

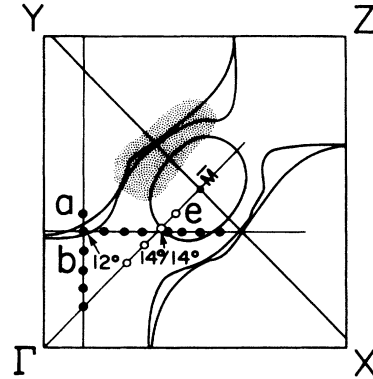


FIG. 2. Section of the calculated Fermi surface of $\text{Bi}_2\text{Sr}_2\text{CoCu}_2\text{O}_8$ (from Ref. 8) showing points at which bands crossing the Fermi level were observed.

The dispersion of this band is shown as the insert of Fig. 1. The band is less steep and the minimum at Γ is closer to E_F than predicted by a one-electron band calculation.⁸ It agrees better with the band structure of a “heavy fermion” state calculated within the formalism of the Anderson lattice model with a large Coulomb interaction U taken into account.¹⁰ The effective mass of this band is estimated to be 2 from our experimental data. A similar increase in mass above the calculated mass was observed by Manzke *et al.*¹¹

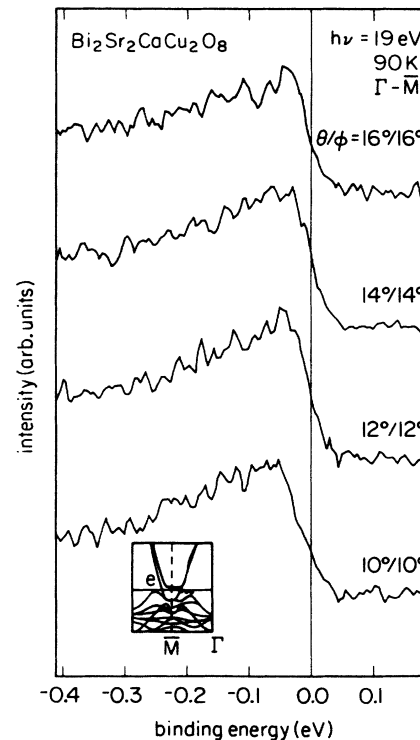


FIG. 3. Angle-resolved energy distribution curves for several angles along the Γ - \bar{M} direction in the Brillouin zone using photons of energy 19 eV. The inset shows the measured band dispersion (dots) and the calculated energy bands of Ref. 8.

One of the tests of the band calculations is whether a band calculated to have Bi-O character crosses the Fermi level, i.e., whether the circular shaped Fermi surface labeled e by Massidda *et al.*⁸ in Fig. 2 exists. To investigate this, we measured EDC's along $\Gamma\text{-}\bar{M}$. The spectra are shown in Fig. 3. (Their corresponding positions in the Brillouin zone are shown as open circles in Fig. 2.) It can be seen that a rather flat band disperses towards the Fermi level, and at 14° the band crosses the Fermi level. As indicated in Fig. 2, this point is exactly on the intersection of $\Gamma\text{-}\bar{M}$ and the circle e . Therefore, it is quite certain that this piece of Fermi surface does exist, although we cannot prove that this part of the Fermi surface has some Bi character, since there is no good Bi resonance that we can use. We note that the measured band is closer to E_F than predicted by Massidda *et al.*⁸ With that adjustment the enhancement of the effective mass is similar to that of the Cu-O band studied in Fig. 1. However, the band near E_F is more complex than the nearly parabolic Cu-O band. An estimate of the effective mass in that region is difficult. Figure 4 shows a series of EDC's taken at 90 K along a line parallel to $\Gamma\text{-}X$ (Fig. 2). Along this line, the density of states near the Fermi level is always quite high. However, if we look more closely, we find that the density of states at the Fermi level decreases on going from $\phi=4^\circ$ to 6° to 8° , indicating the departure of the band from the Fermi level. At 10° and above, the density of states at the Fermi level increases

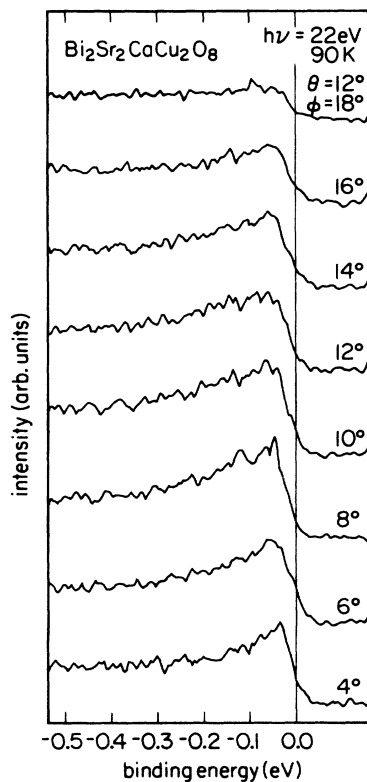


FIG. 4. Angle-resolved energy distribution curves for several angles along the $\Gamma\text{-}X$ direction in the Brillouin zone using photons of energy 22 eV.

again. Another scan in the direction parallel to the scan of Fig. 4 did not resolve the question of the nature of the bands below E_F . The Fermi surface crossing is consistent with Fig. 2. Near point e in Fig. 2 the bands are so close to E_F that they are not clearly resolved. With our resolution it is not possible to show whether the Fermi surface section centered on \bar{M} is or is not connected to the sections centered on X or Y , and whether the band through this region has its minimum at Γ or \bar{M} .

Since the structure of $\text{Bi}_2\text{Sr}_2\text{CaCu}_2\text{O}_8$ is quasitragonal, we would expect similar band dispersion along $\Gamma\text{-}X$ and $\Gamma\text{-}Y$. The corresponding band was seen along $\Gamma\text{-}X$, but it was necessary to use 19 eV photons. The photon beam is almost completely polarized, and selection rules and electric dipole matrix element effects are dramatic. A second crystal was mounted rotated 90° about the c axis from the first. This time the $\Gamma\text{-}X$ band was easily seen at 22 eV, but not at 19 eV, verifying the dipole matrix elements as the cause of the anisotropy.

To summarize, we have observed band dispersion along major symmetry lines and the main features of the Fermi surface are obtained. The agreement between the experiment and the band calculations of the Fermi surface is surprisingly good. The existence of a Fermi surface, the large band dispersion with effective masses enhanced by correlation effects, and the strong dipole matrix element effects all strongly support a Fermi-liquid description of this material.

The fact that the one-electron band calculation is successful in predicting the Fermi surface, but failed to give an accurate band dispersion, is not contradictory. If this system is a true Fermi liquid, Luttinger's theorem¹² should be obeyed, which means the Fermi volume is invariant under interaction effects. Therefore, unless there is a strong anisotropic potential, the Fermi surface should be preserved.

B. Photohole lifetime widths

The peak widths and line shapes of the spectra in Fig. 1 need more attention. Generally, the peak widths are determined by the inverse lifetime of both photoelectrons and holes, in addition to the contributions from instrument resolution. However, for a two-dimensional system, only the hole lifetime contributes to the broadening; the lifetime of the emitted electron does not broaden the peak.¹³⁻¹⁵ Holes at the Fermi level have practically infinite lifetimes. Away from the Fermi level, for a normal Fermi liquid, the inverse hole lifetime increases as $(E - E_F)^2$ in all dimensionalities. There are other possibilities. Recently, a linear dependence on $|E - E_F|$ has been suggested for a "near" Fermi-liquid model,¹⁶ and Fermi surface nesting has been shown to predict such a dependence.¹⁷ Finally, another model exists which accounts for many of the features of our data: dispersion of peaks in the EDC's and the widths of these peaks.¹⁸ The modified single-particle band structure has been successful in describing the data to this point, however, and we will discuss Fig. 1 in this context.

A discussion of the broadening in Fig. 1 is complicated by the finite angular resolution. For the 10° spectrum,

the peak width is determined by our k resolution. [The energy broadening caused by k resolution at this k point is about 84 meV, using the equation $\Delta E = (dE/dk)\Delta k$. dE/dk is estimated from the experimental data.] For the 12° spectrum the measured peak is narrower because only part of the sampled band is filled. As the band moves below the Fermi level, the width increases rapidly. Below 350 meV, the peak became too broad to be distinguished from the background. The asymmetry of the peak is another consequence of the finite angular resolution. There is a significant change in photohole lifetime from one side of our angular acceptance to the other.

We modeled this effect by assuming the angular acceptance function was a square function. Its 2° full width was converted to a width in k_{\parallel} , then to a width in energy via the measured dispersion of the band. The spectrum was simulated by a series of 200 equally spaced Lorentzians throughout the corresponding energy range each with a width of $\alpha|E - E_F|$ or $\beta(E - E_F)^2$. These were summed, then multiplied by the Fermi function and convoluted with the part of the instrument resolution not arising from the finite angular acceptance. For any single spectrum, a value of α or β could be found that gave a fit. However, upon going to other angles and repeating the analysis with the same values of α and β , the quadratic energy dependence of the width gave EDC's that were much more asymmetric than the measured ones, while the linear energy dependence gave a good fit. The best value of α was 0.6 (dimensionless). Replacing the rectangular angle resolution function by a Gaussian gave essentially the same results. The effectively linear dependence of inverse photohole lifetime on energy is consistent with the predictions of Refs. 16 and 17.

The resulting fits, using a linear energy-dependent broadening, are shown in Fig. 5. The data are from Fig. 1 with a background removed. The background at a given binding energy was taken to be proportional to the sum of the primaries at higher kinetic energies. The same constant was used for all spectra. The success of this background method implies that there is a difference between primary and secondary electrons of the same kinetic energy. There is a consistent physical picture in this case if the background is composed of primary electrons that have suffered a small energy loss and small change in momentum at or near the surface. It is very unlikely that electrons with multiple losses will appear in the energy window of these spectra, and the conventional secondary electrons appear at much lower kinetic energies.

The background determined by this method for the 12° spectrum in Fig. 1 is exactly the measured 14° spectrum. There are no filled states at E_F for the momentum corresponding to 14° within the angular acceptance at our analyzer. The photoelectrons we detect have been scattered into the analyzer acceptance with small changes in momentum and small energy loss. Hence there is no emission at E_F (the highest kinetic energy), and the scattered electron spectra are equivalent over a small range of angles. In general points in the zone there are no filled states at E_F and the background is much lower. For example, this background term contributes very little to the

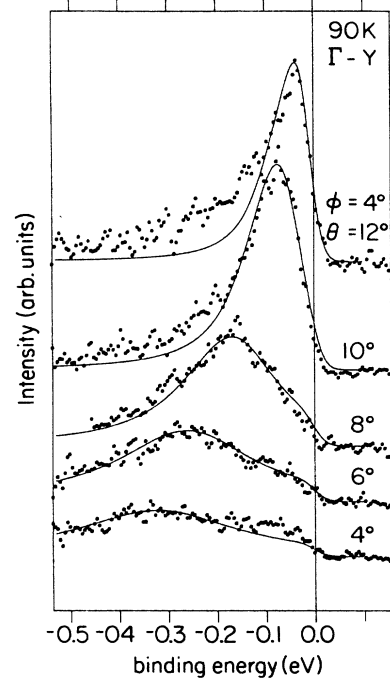


FIG. 5. Spectra of Fig. 1 with background removed. The lines are the fits using a linear energy-dependent broadening as described in the text.

4° spectrum of Fig. 1 (see also Fig. 3 of Ref. 3). On the other hand, the backgrounds are universally high for the spectra in Fig. 4. Throughout this part of the zone, there are occupied states at or near the Fermi level. Scattering events with small energy and momentum changes result in a sizable, almost energy-independent background. These are probably electron-phonon scattering events, rather than the electron-electron scattering events that appear at greater energy loss. We are left with a picture in which the spectra are a result of conventional band dispersion through the Fermi level.

C. Temperature dependence of the Fermi edge

To examine more closely the nature of the states at the Fermi level, an EDC was measured at a point in the Brillouin zone where a band crossed the Fermi level. This point was along the line $\Gamma-\bar{M}$, and was in a region where the one-electron band calculation predicts that these electrons are mixed O $2p$ and Bi $6p$ in character.^{8,9} Then an EDC was taken at the Fermi edge of a clean Pt foil adjacent to the sample. Such spectra taken at several temperatures between 100 and 250 K are shown in Fig. 6, after suitable normalization. The stability of the observed Fermi energy in Pt for scans taken over several days was about 5 meV.

It is clear that the Fermi edges of the two materials agree at all temperatures shown. We see that the apparent Fermi energies are the same within the 5 meV stability of our electron spectrometer. This is the expectation if the material is a Fermi liquid. The resonating valence bond (RVB) model prediction may be different.

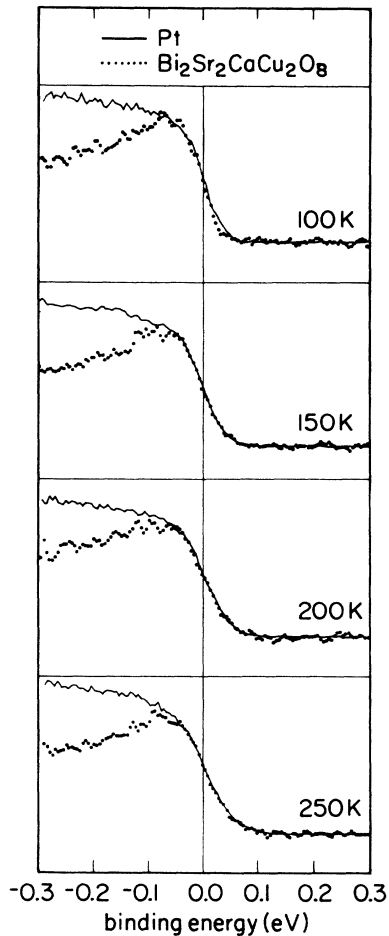


FIG. 6. Comparison of the Fermi edge of Pt with that of $\text{Bi}_2\text{Sr}_2\text{CaCu}_2\text{O}_8$ at several temperatures between 100 and 250 K. The plots have been normalized vertically, but not shifted horizontally.

To explore this question, Huber¹⁹ has made a number of simplifying assumptions, the most important of which is that instead of a photohole, a photoemission event results in the creation of a spinon and a holon which are uncoupled (or very weakly coupled). They share the energy the photohole would have. The result of Huber's calculation is that above T_c there is an edge resembling a Fermi edge. As the temperature increases, the slope of the edge diminishes while the threshold shifts but little.²⁰ The effect is that the midpoint, which might be identified with an apparent Fermi level, shifts to lower energies. This effect

is large if the maximum spinon energy is large. Thus, if the shift of the apparent Fermi energy with temperature is small, the maximum spinon energy is small. The upper bound on the shift is 5 meV.

One should note that Huber's calculation is of the density of states or spectral density in energy for an isotropic material, while our experiment samples only a small region of reciprocal space, i.e., our EDC is effectively a density of states in k space. However, we have looked at several other points in the Brillouin zone at 90 K, points with different atomic character, and see no shift of the apparent Fermi energy when compared with that of Pt, again with an uncertainty of about 5 meV.

In the strong-coupling limit the holon-spinon pair would resemble a quasielectron, and the edge should look like that expected for the Fermi-Dirac distribution function. No calculations of photoemission spectra exist for intermediate coupling strength, but any such calculations are constrained by experiment to closely resemble the Fermi liquid picture.

IV. CONCLUSIONS

In conclusion, we see occupied states at the Fermi level in a relatively small area of the Brillouin zone. These areas are consistent with the calculated Fermi surface. In the normal state, this occupied density is indistinguishable from a normal metal. Away from the Fermi level, bands are heavier than one-electron bands, probably the result of correlation effects. A model starting from single-particle bands is able to explain many features of the spectra. The linear dependence of the photohole widths with energy below E_F may or may not be derived from single-particle theory.

ACKNOWLEDGMENTS

We would like to thank J. Yu and A. J. Freeman for the calculation of the bands above the Fermi level for us. The Ames Laboratory is operated for the U.S. Department of Energy (USDOE) by Iowa State University under Contract No. W-7405-ENG-82. The Argonne National Laboratory is operated for USDOE under Contract No. W-31-109-ENG-38. The Synchrotron Radiation Center is supported by the National Science Foundation (NSF) under Contract No. DMR8601349. Y.C.C. acknowledges support from NSF—Office of Science and Technology Centers under Contract No. STC-8809854 (Science and Technology Center for Superconductivity—University of Illinois-Urbana-Champaign).

¹P. W. Anderson, *Science* **235**, 1196 (1987).

²R. B. Laughlin, *Science* **242**, 525 (1988).

³C. G. Olson, R. Liu, D. W. Lynch, B. W. Veal, Y. C. Chang, P. Z. Jiang, J. Z. Liu, A. P. Paulikas, A. J. Arko, and R. S. List, *Physica C* **162-164**, 1697 (1989).

⁴Cleaving apparently results in a Bi-O surface plane. See P. A. Lindberg *et al.*, *Phys. Rev. B* **39**, 2890 (1989).

⁵A. J. Arko, R. S. List, Z. Fisk, S.-W. Cheong, J. D. Thompson,

J. A. O'Rourke, C. G. Olson, A.-B. Yang, Tun-Wen Pi, J. E. Schirber, and N. D. Shinn, *J. Magn. Magn. Mater.* **75**, L1 (1988).

⁶R. S. List, A. J. Arko, Z. Fisk, S.-W. Cheong, S. D. Conradson, J. D. Thompson, C. B. Pierce, D. E. Peterson, R. J. Bartlett, J. A. O'Rourke, N. D. Shinn, J. E. Schirber, C. G. Olson, A.-B. Yang, T.-W. Pi, B. W. Veal, A. P. Paulikas, and J. C. Cam-puzano, *J. Vac. Sci. Technol.* (to be published).

- ⁷C. G. Olson, *Nucl. Instrum. Methods* **A266**, 205 (1988).
- ⁸S. Massidda, J. Yu, and A. J. Freeman, *Physica C* **52**, 251 (1988).
- ⁹H. Krakauer and W. E. Pickett, *Phys. Rev. Lett.* **60**, 1665 (1988).
- ¹⁰P. C. Pattnaik and D. M. Newns, *Phys. Rev. B* **41**, 880 (1990).
- ¹¹R. Manzke, T. Buslaps, R. Claessen, M. Skibowski, and J. Fink, *Physica C* **162-164**, 1381 (1989).
- ¹²J. M. Luttinger, *Phys. Rev.* **119**, 1153 (1960).
- ¹³J. B. Pendry, in *Photoemission and the Electronic Properties of Surfaces*, edited by B. Feuerbacher, B. Fitton, and R. F. Willis (Wiley, New York, 1978), p. 94.
- ¹⁴T. C. Chiang, J. A. Knapp, M. Aono, and D. E. Eastman, *Phys. Rev. B* **21**, 3515 (1980).
- ¹⁵B. J. Slagvold, J. K. Grepstad, and P. O. Gartland, *Phys. Scr.* **T4**, 65 (1983).
- ¹⁶C. M. Varma, P. B. Littlewood, S. Schmitt-Rink, E. Abrahams, and A. E. Ruckenstein, *Phys. Rev. Lett.* **63**, 1996 (1989).
- ¹⁷A. Virosztek and J. Ruvalds (unpublished).
- ¹⁸P. W. Anderson, *Phys. Rev. Lett.* **64**, 1839 (1990); and (private communication).
- ¹⁹D. L. Huber, *Solid State Commun.* **68**, 459 (1988).
- ²⁰Y. Chang, M. Tang, Y. Hwu, M. Onellion, D. L. Huber, G. Margaritondo, P. A. Morris, W. A. Bonner, J. M. Tarascon, and N. G. Stoeffel, *Phys. Rev. B* **39**, 7313 (1989).

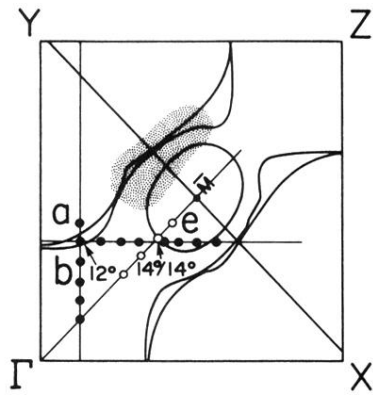


FIG. 2. Section of the calculated Fermi surface of $\text{Bi}_2\text{Sr}_2\text{CaCu}_2\text{O}_8$ (from Ref. 8) showing points at which bands crossing the Fermi level were observed.